Thermally stimulated currents due to multiple-trapping carrier transport. I. Gaussian transport

1992 J. Phys.: Condens. Matter 4 3967

(http://iopscience.iop.org/0953-8984/4/15/012)

J. Phys.: Condens. Matter 4 (1992) 3967–3984. Printed in the UK

Thermally stimulated currents due to multiple-trapping carrier transport: I. Gaussian transport

W Tomaszewicz
Laboratory of Organic Dielectrics and Semiconductors, Technical University of Gdańsk, Majakowskiego 11/12, 80-952 Gdańsk, Poland

Received 4 November 1991

Abstract. Non-isothermal carrier transport in an insulator with trapping states is studied for the case of approximate thermal equilibrium between free and trapped carriers. The temperature dependences of the trap parameters and of the microscopic carrier mobility are taken into account. It is shown that the carrier packet in the sample has a Gaussian shape, independently of the form of the energetic trap distribution. On this basis, a simple formula describing thermally stimulated currents (TSC) is obtained. Its accuracy is estimated by comparison with the results of Monte Carlo calculations for model trap distributions. Methods of determining the trap parameters from the measured TSC curves are considered.

1. Introduction

Measurements of thermally stimulated currents (TSC) are a useful and widely applied technique in the study of trap levels in insulators and semiconductors. In the conventional theory of TSC (e.g. [1–4]), it is assumed that the TSC course is determined uniquely by the processes of carrier trapping/detrapping and recombination. The time variation of the spatial carrier distribution in the sample during measurements is disregarded. As a consequence, the theory predicts that the shape and the position of the TSC peak on the temperature scale depend, aside from material parameters, entirely on the heating rate.

Since the mid-1970s another theory of TSC has been developed, which takes into account explicitly the movement of the carrier packet in the sample. It is presupposed that a thin sheet of excess carriers is initially generated by light, ionizing radiation, etc, near one of the sample surfaces. With increase of the sample temperature, carriers of one sign are quickly neutralized on the nearer electrode. Carriers of opposite sign drift through the whole sample thickness under the action of the external field applied to the sample. Carrier recombination occurs only up to complete separation of carriers of opposite sign. The initial rise of the current is then due to an increase in the carrier packet velocity, while the subsequent decay is caused by carrier neutralization at the collecting electrode.

The described 'TSC drift experiment' is analogous to isothermal measurement of the carrier time of flight (TOF). For this reason, the development of its theoretical description has been stimulated by achievements in the theory of the TOF method [5–11]. Similarly to the isothermal case, two basic mechanisms of carrier transport—multiple trapping [12–18] and hopping [19, 20]—have been considered, for both non-dispersive as well as

0953-8984/92/153967 + 18 $04.50

dispersive transport regimes. Among other things, it was shown that the shape of the TSC curve and the temperature for which the maximum of the TSC peak occurs should depend not only on the heating rate but also on the sample thickness and the field strength (even if high-field effects, such as the Poole–Frenkel one, are absent). This prediction was verified experimentally for poly(*N*-vinylcarbazole) [21], polyphenylquinoxaline [22] and crystalline anthracene doped with phenothiazine [23]. Recently, 'TSC drift measurements' were carried out for polymethylphenylsilane [24, 25].

In spite of considerable progress, the mentioned theory of TSC is still incomplete. As regards non-dispersive multiple-trapping transport, the general formula describing TSC was derived solely for the case of a single trapping level [16]. Some results concerning this case were obtained earlier by Samoć and Samoć [12] and Plans *et al* [13]. For traps distributed in energy, only formulae determining the initial rise and the maximum temperature of TSC have been obtained up till now [14]. Moreover, in all the previous research the temperature dependences of carrier mobility and of some trap parameters were disregarded. The present work aims to give a full analytical description of TSC in the considered case, as well as numerical verification of the formulae obtained. In a following paper (II), some new analytical and numerical results on dispersive multiple-trapping TSC are presented.

2. Formulation of the problem

2.1. Basic assumptions

In the multiple-trapping model the carriers are assumed to move in the conduction (or valence) band, being temporarily immobilized in traps situated in the energy gap. According to the conditions of the 'TSC drift experiment' excess carrier transport of only one sign is considered. The density of these carriers is assumed to exceed significantly the equilibrium density of thermally generated carriers (the case of an insulating solid). On the other hand, the excess carrier density should be small enough to ensure the uniformity of the electric field in the sample (the small-signal case) as well as negligible trap occupancy. The last condition implies that the carrier capture probability is independent of the density of trapped carriers. Moreover, carrier diffusion is neglected, which is justified for sufficiently high fields. Unlike the previous papers, we take into account the temperature dependences of the microscopic carrier mobility, the carrier capture coefficient and the frequency factor. These parameters are time-dependent in the case of non-isothermal transport.

2.2. Transport equations

We shall assume that carrier transport takes place along the direction of the x axis, perpendicular to the sample surfaces positioned at $x = 0$ and $x = d$ (d = sample thickness). In order to simplify the formulae, the new space variable $z = x/\mu_0 E$ is introduced, where μ_0 is the free-carrier mobility at the initial moment ($t = 0$) and E is the electric field strength. The free- and trapped-carrier densities are denoted by $n(z, t)$ and $n_t(z, t)$, respectively. The density of carriers per unit energy in traps of depth ε is denoted by $n_t'(z, t, \varepsilon)$. Then the equations governing carrier transport are [13, 14]

$$\partial[n(z,t) + n_t(z,t)]/\partial t + u(t)\,\partial n(z,t)/\partial z = 0 \tag{1}$$

$$\partial n_t'(z,t,\varepsilon)/\partial t = C_t(\varepsilon,t)N_t(\varepsilon)n(z,t) - n_t'(z,t,\varepsilon)/\tau_r(\varepsilon,t) \tag{2}$$

$$n_t(z, t) = \int_{\varepsilon_t^0}^{\varepsilon_t} n_t'(z, t, \varepsilon)\, d\varepsilon. \tag{3}$$

Here $u(t) = \mu(t)/\mu_0$, where $\mu(t)$ is the microscopic carrier mobility, $C_t(\varepsilon, t)$ is the carrier capture coefficient, $N_t(\varepsilon)$ is the trap density per unit energy, ε_t^0 and ε_t are the limits of the trap distribution, and finally $\tau_r(\varepsilon, t)$ is the mean lifetime of the trapped carrier, given by

$$\tau_r(\varepsilon, t) = \nu^{-1}(\varepsilon, t) \exp[\varepsilon/kT(t)] \tag{4}$$

with $\nu(\varepsilon, t)$ = frequency factor, k = Boltzmann constant and $T(t)$ = sample temperature. The energy ε is measured from the edge of the conduction (valence) band. The frequency factor and the carrier capture coefficient are interrelated by the detailed equilibrium principle:

$$\nu(\varepsilon, t) = C_t(\varepsilon, t) N_{eff}(t) \tag{5}$$

where $N_{eff}(t) \propto T^{3/2}(t)$ stands for the effective density of states in the conduction (valence) band. Equation (1) is the continuity equation while equation (2) describes the kinetics of carrier trapping/detrapping.

Equations (2) and (3) can be transformed to a more compact form [14]. Integrating equation (2) by turns with respect to t and ε variables, taking into account equation (3), and setting $n_t'(z, 0, \varepsilon) = 0$, one obtains

$$n_t(z, t) = \int_0^t \Phi(t, t') n(z, t')\, dt' \tag{6}$$

where the function

$$\Phi(t, t') = \int_{\varepsilon_t^0}^{\varepsilon_t} C_t(\varepsilon, t') N_t(\varepsilon) \exp\left(-\int_{t'}^{t} \frac{dt''}{\tau_r(\varepsilon, t'')}\right) d\varepsilon. \tag{7}$$

The above formulae have a simple interpretation. The function $\Phi(t, t')$ determines the probability that a carrier that is free at time t' is trapped in a time unit and remains in the trap until time t. The integrand in equation (6) represents, therefore, the density of carriers captured within the time interval $(t', t' + dt')$ and remaining in the traps until time t.

The current intensity $I(t)$ induced in the external circuit by carrier motion is equal to the conduction current intensity in the sample averaged over its thickness (e.g. [8]). In our notation

$$I(t) = \frac{I_0 u(t)}{n_0 \tau_0} \int_0^{\tau_0} n(z, t)\, dz \tag{8}$$

where $I_0 = en_0\mu_0 ES$ is the initial current intensity (e = elementary charge, n_0 = density of generated carriers, averaged over sample thickness, S = sample cross-sectional area) and $\tau_0 = d/\mu_0 E$ is the trap-free time of flight, corresponding to the initial temperature.

2.3. *Thermal equilibrium approximation*

From the initial moment of their generation, the carriers redistribute themselves between the conduction (valence) band and the trap levels. Finally, approximate thermal equilibrium between free and trapped carriers is established. In what follows, we assume

that the time for carrier thermalization is short compared to the considered timescale, which implies that $t \gg \tau_r(\varepsilon, t)$ for an arbitrary trap level. In such a case, equation (6) describing the trapping/detrapping kinetics can be simplified. It is seen that the integral in the exponential factor in (7) is then much larger than unity, except for $t' \simeq t$. Thus, the function $\Phi(t, t')$ differs significantly from zero only for a very small difference of the arguments. The free-carrier density in equation (6) can then be replaced by the initial terms of its Taylor series,

$$n(z, t') \simeq n(z, t) - (t - t')\frac{\partial n(z, t)}{\partial t} \tag{9}$$

which results in the equation

$$n_t(z, t) \simeq \frac{[1 - \Theta(t)]}{\Theta(t)} n(z, t) - \tau_s(t)\frac{\partial n(z, t)}{\partial t} \tag{10}$$

where

$$\Theta^{-1}(t) = 1 + \int_0^t \Phi(t, t')\,dt' \tag{11}$$

$$\tau_s(t) = \int_0^t (t - t')\Phi(t, t')\,dt'. \tag{12}$$

The last term in equation (10) approximately takes into account the deviations of the free- and trapped-carrier densities from their equilibrium values. This results from the fact that equation (10), with the last term omitted, can be obtained by setting $\partial n_t'(z, t, \varepsilon)/\partial t = 0$ in equation (2), i.e. by assuming exact thermal equilibrium [14].

To calculate the above integrals we use the following formula for the integral in equation (7):

$$\int_{t'}^{t} \frac{dt''}{\tau_r(\varepsilon, t'')} \simeq \frac{t - t'}{\tau_r(\varepsilon, t)} \tag{13}$$

which is valid for only slightly differing integration limits, and replace $C_t(\varepsilon, t')$ by $C_t(\varepsilon, t)$. Taking into account the inequality $t \gg \tau_r(\varepsilon, t)$, $\varepsilon_t^0 \leqslant \varepsilon \leqslant \varepsilon_t$, one obtains

$$\Theta^{-1}(t) \simeq 1 + \int_{\varepsilon_t^0}^{\varepsilon_t} C_t(\varepsilon, t)N_t(\varepsilon)\tau_r(\varepsilon, t)\,d\varepsilon \tag{14}$$

$$\tau_s(t) \simeq \int_{\varepsilon_t^0}^{\varepsilon_t} C_t(\varepsilon, t)N_t(\varepsilon)\tau_r^2(\varepsilon, t)\,d\varepsilon. \tag{15}$$

These formulae can be rewritten in a clearer form. Introducing the free-carrier lifetime $\tau_t(t)$, given by

$$\tau_t^{-1}(t) = \int_{\varepsilon_t^0}^{\varepsilon_t} C_t(\varepsilon, t)N_t(\varepsilon)\,d\varepsilon \tag{16}$$

and denoting by a bar the averaging over energy with the weight $C_t(\varepsilon, t)N_t(\varepsilon)$, we have

$$\Theta(t) \simeq \frac{\tau_t(t)}{[\tau_t(t) + \overline{\tau}_r(t)]} \tag{17}$$

$$\tau_s(t) \simeq \frac{\overline{\tau_r^2}(t)}{\tau_t(t)}. \tag{18}$$

The function $\Theta(t)$ is therefore approximately equal to the mean time fraction at which the carrier remains free, corresponding to moment t. In the case of fast trapping, when $\tau_t(t) \ll \overline{\tau_r}(t)$, the value $\Theta(t) \simeq \tau_t(t)/\overline{\tau_r}(t) \ll 1$.

The formulation of the initial condition for the system of equations (1) and (10) encounters some difficulties, because equation (10) is valid only after carrier thermalization. We assume that the mean distance travelled by the carrier up to this time is much shorter than the sample thickness, and that the relation between free and trapped carriers is then given by equation (10), with the last term on the RHS dropped. In such a case

$$n(z,0) = n_0 \tau_0 \Theta(0) \delta(z) \tag{19}$$

with $\delta(z)$ = Dirac delta function, where for simplicity the time of carrier thermalization is set to zero.

3. Analytical results

3.1. Solution of transport equations

By eliminating the trapped-carrier density from equations (1) and (10) we obtain the second-order differential equation describing the evolution of the free-carrier density:

$$\frac{\partial}{\partial t}\left(\frac{n(z,t)}{\Theta(t)}\right) + u(t)\frac{\partial n(z,t)}{\partial z} - \frac{\partial}{\partial t}\left(\tau_s(t)\frac{\partial n(z,t)}{\partial t}\right) \simeq 0. \tag{20}$$

This equation does not seem to have a simple analytical solution and some further approximations are necessary. Assuming the last term in equation (20) to be small compared to the other ones, the perturbation method can be applied. Ignoring that term for a moment, one gets

$$\frac{\partial}{\partial t}\left(\frac{n(z,t)}{\Theta(t)}\right) \simeq -u(t)\frac{\partial n(z,t)}{\partial z}. \tag{21}$$

Making use of this equation, the time derivatives of the function $n(z,t)$ in the last term in (20) can be expressed by the function $n(z,t)$ itself and by its space derivatives. Retaining only the term that contains the second-order space derivative, we find

$$\frac{\partial}{\partial t}\left(\frac{n(z,t)}{\Theta(t)}\right) + u(t)\frac{\partial n(z,t)}{\partial z} - \tau_s(t)\Theta^2(t)u^2(t)\frac{\partial^2 n(z,t)}{\partial z^2} \simeq 0. \tag{22}$$

It may be checked that all the omitted terms are small compared to the first or the second terms in (22), provided that the function $\tau_s(t)$ and its time derivative assume sufficiently small values.

Equation (22) can be integrated after the following change of variables, $n(z,t) = \Theta(t)n^*[y(z,t), \xi(t)]$, where

$$y(z,t) = z - \zeta(t) \tag{23}$$

$$\zeta(t) = \int_0^t \Theta(t')u(t')\,dt' \tag{24}$$

$$\xi(t) = \int_0^t \tau_s(t')\Theta^3(t')u^2(t')\,dt'. \tag{25}$$

The resulting equation has the form of a diffusion equation in one dimension,

$$\partial n^*(y, \xi)/\partial\xi - \partial^2 n^*(y, \xi)/\partial y^2 \simeq 0 \tag{26}$$

while the initial condition (19) turns out to be

$$n^*(y, 0) \simeq n_0\tau_0\delta(y). \tag{27}$$

Using the elementary solution of the diffusion equation (e.g. [26]), we get

$$n^*(y, \xi) = [n_0\tau_0/2(\pi\xi)^{1/2}]\exp(-y^2/4\xi). \tag{28}$$

Returning to the original variables, we find the expression determining the free-carrier density:

$$n(z, t) = \frac{n_0\tau_0\Theta(t)}{2[\pi\xi(t)]^{1/2}}\exp\left(-\frac{[z - \zeta(t)]^2}{4\xi(t)}\right). \tag{29}$$

The trapped-carrier density can be calculated now from equation (10). Omitting the term that contains $\tau_s(t)$, we obtain

$$n_t(z, t) = \frac{n_0\tau_0[1 - \Theta(t)]}{2[\pi\xi(t)]^{1/2}}\exp\left(-\frac{[z - \zeta(t)]^2}{4\xi(t)}\right). \tag{30}$$

Thus, under our approximations, the carrier packet has a Gaussian shape. The 'centroid' and the RMS spread of the carrier packet are given by the formulae $\langle z(t)\rangle = \zeta(t)$ and $\sigma(t) = [2\xi(t)]^{1/2}$, respectively. If the relative dispersion of the carrier packet $\sigma(t)/\langle z(t)\rangle$ tends to zero, the formulae (29) and (30) reduce to those obtained in [14] under the assumption of exact thermal equilibrium between free and trapped carriers. This proves that the finite spread of the carrier packet originates from incomplete carrier thermalization.

The resulting TSC can be calculated by inserting the free-carrier density (29) into integral (8). Replacing the lower limit of integration by $-\infty$, which is justified when the ratio $\xi^{1/2}(t)/\zeta(t) \ll 1$, we obtain

$$I(t) = \frac{I_0\Theta(t)u(t)}{2}\left[1 + \operatorname{erf}\left(\frac{\tau_0 - \zeta(t)}{2\xi^{1/2}(t)}\right)\right] \tag{31}$$

where erf(...) is the error function. As follows from this formula, the initial rise of the TSC and the time τ_e corresponding roughly to the TSC maximum are given by

$$I_{in}(t) = I_0\Theta(t)u(t) \tag{32}$$

$$\zeta(\tau_e) = \tau_0. \tag{33}$$

Equation (33) shows that the time τ_e corresponds to the effective carrier transit time across the sample. The formulae (29)–(33) are quite general. As may be checked, they reproduce all the partial results obtained previously [12–14, 16]. Because of numerous approximations, it is difficult to give the precise conditions under which the derived formulae are reliable. However, one can expect their accuracy to improve as the carrier densities approach the equilibrium values, i.e. as the relative dispersion of the carrier packet decreases. Thus, formulae (29) and (30) and formula (31) should be accurate for small values of the ratios $\xi^{1/2}(t)/\zeta(t)$ and $\xi^{1/2}(\tau_e)/\tau_0$, respectively.

In this paper, we deal mainly with the case of carrier generation at the sample surface. One can also obtain solutions of the transport equation (22) corresponding to carrier generation in the whole sample volume. However, such solutions seem to be of less interest. Since carriers of both sign are then generated in the sample, their applicability is restricted to the case of negligible carrier recombination during the whole TSC run. In general, transport of both positive and negative carriers would then contribute to the measured current, which makes the TSC analysis more difficult. Some formulae corresponding to uniform carrier generation in the sample are given in appendix 1.

3.2. Discussion

In order to study the main features of the TSC, we have to specify the mode of sample heating, the temperature dependences of the transport and trap parameters, as well as the form of the trap distribution. We assume that the sample temperature increases linearly in time:

$$T(t) = T_0 + \beta t \tag{34}$$

with T_0 = initial temperature, β = heating rate. Such a heating scheme is commonly used in TSC measurements. In what follows, all the time-dependent functions are expressed in terms of the sample temperature.

The temperature dependence of the free-carrier mobility can be approximated in a limited temperature range by $\mu(T) \propto T^a$, where the parameter a depends on the carrier scattering mechanism. In the case of covalent semiconductors, for scattering on acoustic phonons and on charged impurities, a equals $-3/2$ and $3/2$, respectively (see e.g. [27]). Thus, we have

$$u(T) = (T/T_0)^a. \tag{35}$$

The temperature dependences of the carrier capture coefficient and the frequency factor have been discussed, for example, by Kivits and Hagebeuk [28]. The corresponding formulae are

$$C_t(T) = C_{t0}(T/T_0)^{1/2-b} \tag{36}$$

$$\nu(T) = \nu_0(T/T_0)^{2-b} \tag{37}$$

where the parameter b depends on the functional shape of the potential energy near the trapping centre ($0 \leqslant b \leqslant 4$). In particular, for neutral and coulombic centres b equals 0 and 2, respectively. Here, the possible energy dependence of $C_t(\varepsilon, T)$ and $\nu(\varepsilon, T)$ is disregarded.

As far as the model trap distributions are concerned, we choose monoenergetic and power distributions in the form

$$N_t(\varepsilon) = N_{tot}\delta(\varepsilon_t - \varepsilon) \tag{38}$$

$$N_t(\varepsilon) = \frac{[(c+1)N_{tot}(\varepsilon_t - \varepsilon)^c]}{(\varepsilon_t - \varepsilon_t^0)^{c+1}} \tag{39}$$

where N_{tot} is the trap density per unit sample volume. The trap distribution (39) includes the special cases of uniform ($c = 0$) and linear ($c = 1$) distributions. To ensure convergence of the integrals in (14) and (15), the condition $c > -1$ must be fulfilled.

With the aid of the above formulae, the functions $\Theta(t)$, $\tau_s(t)$, $\zeta(t)$ and $\xi(t)$ can be approximately calculated (appendix 2). Below, only the final formulae are given, which

describe the initial TSC rise, the temperature $T_e = T(\tau_e)$ corresponding to the maximum of the TSC, as well as the $\xi(T_e)/\tau_0^2$ ratio. The latter quantity is proportional to the square of the relative dispersion of the carrier packet at temperature T_e. For a single trapping level (38) one obtains

$$I_{in}(T) = \frac{Q_0 \tau_{t0} \nu_0}{\tau_0} \left(\frac{T}{T_0}\right)^{a+3/2} \exp\left(-\frac{\varepsilon_t}{kT}\right) \tag{40}$$

$$T_e^{-1} \simeq \frac{k}{\varepsilon_t} \ln\left[\frac{\tau_{t0}\nu_0 k T_0^2}{\varepsilon_t \beta \tau_0}\left(\frac{T_e}{T_0}\right)^{a+7/2}\right] \tag{41}$$

$$\frac{\xi(T_e)}{\tau_0^2} \simeq \frac{\tau_{t0}}{\tau_0}\left(\frac{T_e}{T_0}\right)^{a+b-1/2} \tag{42}$$

while for a power trap distribution (39) one gets

$$I_{in}(T) \simeq \frac{Q_0 \tau_{t0} \nu_0}{\Gamma(c+2)\tau_0}\left(\frac{T_c}{T_0}\right)^{c+1}\left(\frac{T}{T_0}\right)^{a-c+1/2} \exp\left(-\frac{\varepsilon_t}{kT}\right) \tag{43}$$

$$T_e^{-1} \simeq \frac{k}{\varepsilon_t} \ln\left[\frac{\tau_{t0}\nu_0 k T_0^2}{\Gamma(c+2)\varepsilon_t \beta \tau_0}\left(\frac{T_c}{T_0}\right)^{c+1}\left(\frac{T_e}{T_0}\right)^{a-c+5/2}\right] \tag{44}$$

$$\frac{\xi(T_e)}{\tau_0^2} \simeq \frac{\tau_{t0}}{\Gamma(c+2)\tau_0}\left(\frac{T_c}{2T_0}\right)^{c+1}\left(\frac{T_e}{T_0}\right)^{a+b-c-3/2}. \tag{45}$$

Here, $Q_0 = I_0\tau_0$ is the initial charge generated in the sample, $\tau_{t0} = \tau_t(T_0)$, $\Gamma(\ldots)$ is the Euler gamma function and the parameter T_c determines the width of the trap distribution (39), $\varepsilon_t - \varepsilon_t^0 = kT_c$. In the calculations it was assumed that $T_c \gg T$. The charge Q_0 equals the area under the TSC curve and is therefore a measurable quantity.

It should be noted that equations (40)–(42) can be obtained from (43)–(45) by setting formally $c = -1$. For this reason, further discussion is based on equations (43)–(45). According to them, the shape of the TSC curve is characterized mainly by the maximum trap depth ε_t, as well as by the form of the trap distribution and the temperature dependence of the microscopic carrier mobility (via parameters c and a, respectively). With suitably chosen parameters, the TSC curves corresponding to a discrete trap level and a power trap distribution may be identical. Thus, the TSC measurements allow us to obtain information about the trap distribution only if the temperature dependence of the free-carrier mobility is known *a priori*. For example, this is the case when the TSC are measured in doped crystalline materials [23]. The shape of the TSC peak is almost insensitive to the temperature dependence of the $C_t(T)$ and $\nu(T)$ functions (to the parameter b), which influences only the degree of carrier packet dispersion, i.e. the TSC course near the maximum. Therefore, in practice no information about the kind of trapping centres can be inferred. One can recognize that the possible energy dependence of $C_t(\varepsilon, T)$ and $\nu(\varepsilon, T)$ also affects solely the dispersion of the carrier packet. This follows from the fact that the integrand in equation (14), determining the function $\Theta(T)$, contains the ratio $C_t(\varepsilon, T)/\nu(\varepsilon, T)$, which is independent of energy (cf. equations (4) and (5)).

According to equations (43) and (44), it is convenient to analyse the TSC data by plotting $\ln I_{in}$ versus T^{-1} and T_e^{-1} versus $\ln(E/\beta d)$. Both plots allow us to determine independently the same quantities, which provides a test of the consistency of the theory. These plots are expected to be almost linear for $\varepsilon_t \gg kT$, since the power functions of T

and T_e on the RHS of equations (43) and (44) then affect the TSC curve only slightly. If the experimental plots reveal some curvature and the value of the parameter a is known, one can determine the parameter c and distinguish between trap distributions (38) and (39). Otherwise, the concrete model of the trap distribution (e.g. single trapping level) must be tentatively assumed. The mentioned plots allow also the calculation of the trap depth ε_t, as well as the product $\tau_{t0}\mu_0\nu_0(T_c/T_0)^{c+1}$. Some additional information can be obtained from the $\xi^{1/2}(T_e)/\tau_0$ ratio, given by equation (45), which characterizes the carrier packet dispersion at the temperature T_e. The value of $\xi^{1/2}(T_e)/\tau_0$ may be determined by fitting the TSC curve with equation (31) (in the first approximation $\xi(T)$ can be replaced by $\xi(T_e)$). Then, one can estimate the product $\tau_{t0}\mu_0(T_c/T_0)^{c+1}$ and the frequency factor ν_0 (the factors $\Gamma(c+2)$ and $(T_e/T_0)^{a+b-c-3/2}$ in (45) should not differ greatly from unity). It follows from equation (45) that the ratio $\xi^{1/2}(T_e)/\tau_0$ is proportional to $(E/d)^{1/2}$, which in principle can be verified experimentally. However, equation (31) has a good accuracy only for small values of $\xi^{1/2}(T_e)/\tau_0$ (see section 4.2). One can note that essentially the same parameters can be found from the TOF measurements in the Gaussian transport regime at different temperatures (cf. [8, 9]).

The above-mentioned features of the TSC are believed to be rather general. The calculations given in appendix 2 imply that the TSC course depends in fact on the shape of the trap distribution in the energy region in the vicinity of the ε_t level (few kT). It is quite possible that the real trap distribution can be approximated by the function (38) or (39) in this range of energies, though this may not be true for some special distributions.

4. Numerical analysis

4.1. Monte Carlo method

The Monte Carlo technique has been utilized many times for simulations of isothermal multiple-trapping carrier transport (e.g. [29, 30]). In the present paper, this method is extended to non-isothermal transport, which enables verification of the accuracy of the formulae describing TSC. Some results of the TSC simulation have already been published [16–18], but the algorithm used has not been described in detail.

As in the isothermal case, the simulation of individual carrier transport consists of calculating repeatedly the following random variables: the free-carrier lifetime Δt_{tr}, the trap depth ε and the carrier dwell-time Δt_r in the trap. The corresponding distribution functions are:

$$F_1(\Delta t_{tr}) = 1 - \exp\left(-\int_{t_{tr}}^{t_{tr}+\Delta t_{tr}} \frac{dt}{\tau_t(t)}\right) = 1 - \exp\left(-\frac{\Delta t_{tr}}{\tau_t(t_{tr})}\right) \tag{46}$$

$$F_2(\varepsilon) = \frac{1}{N_{tot}} \int_{\varepsilon_t^0}^{\varepsilon} N_t(\varepsilon')\, d\varepsilon' \tag{47}$$

$$F_3(\Delta t_r) = 1 - \exp\left(-\int_{t_r}^{t_r+\Delta t_r} \frac{dt}{\tau_r(\varepsilon, t)}\right). \tag{48}$$

Here, t_{tr} and t_r are the moments of carrier emission from the traps and of carrier capture, respectively. The approximation used in equation (46) follows from the fact that in the present calculations $\Delta t_{tr} \ll t_{tr}$. According to the known theorem (e.g. [31]), the values of Δt_{tr}, ε and Δt_r can be obtained by equating the above functions to random numbers

X', X'' and X''', uniformly distributed in the interval (0, 1), and solving the resulting equations. The calculations are carried out for the discrete trap level (38) and the uniform trap distribution, i.e. the distribution (39) with $c = 0$. Then, one obtains

$$\Delta t_{tr} = -\tau_t(t_{tr}) \ln(X') \tag{49}$$

$$\varepsilon = \varepsilon_t^0 + kT_e X'' \tag{50}$$

$$\int_{t_r}^{t_r+\Delta t_r} \frac{dt}{\tau_r(\varepsilon, t)} = -\ln(X'''). \tag{51}$$

Equation (50) concerns the uniform distribution of traps; for the monoenergetic trapping level, $\varepsilon = \varepsilon_t$. Equation (51), determining the time Δt_r, is solved numerically as described in appendix 3.

The free-carrier displacement and the resulting current, flowing in the external circuit from t_{tr} to $t_{tr} + \Delta t_{tr}$, are given by $\Delta z \simeq u(t_{tr})\Delta t_{tr}$ and $I_e = e/\tau_0$, respectively. In the first equation, the variation of the function $u(t)$ in the time interval Δt_{tr} is disregarded, since $\Delta t_{tr} \ll t_{tr}$. For surface carrier generation, the initial position of the carrier is $z_0 = 0$. For uniform carrier generation in the sample, the initial position is calculated from $z_0 = \tau_0 X^0$ (X^0 = random number of the uniform distribution in (0, 1)). The motion of the single carrier is terminated when it reaches the opposite surface ($z = \tau_0$) of the sample or, alternatively, when the carrier dwell-time in the sample exceeds the given final value. The TSC curve is obtained by repeating this procedure for a large number N of carriers and averaging the induced current. Since the carrier position, as well as the depth of the trap capturing the carrier, are monitored in the program, one can also obtain the spatial and energetic carrier distributions at given times.

4.2. Comparison between analytical and numerical results

The TSC peaks calculated with the aid of the Monte Carlo method are presented in figures 1 and 2 (points). The initial TSC spike occurring in the figures is an artifact. It results from averaging of the large initial current pulse $I(t) \simeq I_0 \exp(-t/\tau_{t0})$, $0 \leqslant t \leqslant \tau_0$ (so-called Hecht term), related to the primary trapping of the generated carriers. For comparison, the TSC curves obtained from approximate formulae (31) and (A1.3) are also shown in the figures (full curves). Several integrals in the equations determining the functions $\Theta(T)$, $\tau_s(T)$, $\zeta(T)$ and $\xi(T)$ cannot be expressed exactly by elementary functions. These integrals were calculated numerically.

Figure 1 shows the results obtained for the monoenergetic trap level for both surface and uniform volume generation of carriers. The TSC curves in figures 1(*a*) and (*b*) are characterized by the same initial rise and the temperature $T_e = T(\tau_e)$, but by different values of the ratio $\xi^{1/2}(T_e)/\tau_0$ (approximately equal to 0.3 and 0.09, respectively). The last quantity determines the extent of carrier thermalization at time τ_e (cf. section 3.1). It is seen that the approximate formulae for TSC become more accurate as the ratio $\xi^{1/2}(T_e)/\tau_0$ decreases, and the accuracy is quite good for $\xi^{1/2}(T_e)/\tau_0 \simeq 0.09$. The TSC peaks calculated for delta-like and uniform initial carrier distributions differ significantly, because in the first case carrier neutralization at the collecting electrode takes place at time $t \simeq \tau_e$, while in the second case it occurs in the time region $0 < t \leqslant \tau_e$.

Figures 2(*a*) and (*b*) illustrate the influence of the temperature dependence of the free-carrier mobility (characterized by the value of the parameter a) on the TSC course for the single trapping level and the uniform trap distribution, respectively. In the

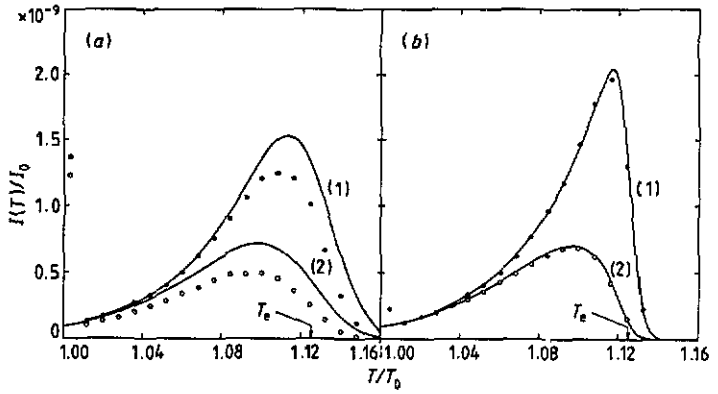

Figure 1. TSC curves calculated for monoenergetic trap level and both surface (1) and volume (2) carrier generation: $\tau_0\beta/T_0 = 10^{-10}$; $\tau_{t0}\beta/T_0 = 10^{-11}$ (a), 10^{-12} (b); $\nu_0 T_0/\beta = 10^{14}$ (a), 10^{15} (b); $\varepsilon_t/kT_0 = 30$; $a = -1.5$; $b = 0$; $N = 10^4$ $(a, 1)$, 2×10^4 $(a, 2)$, 10^3 $(b, 1)$, 2×10^3 $(b, 2)$.

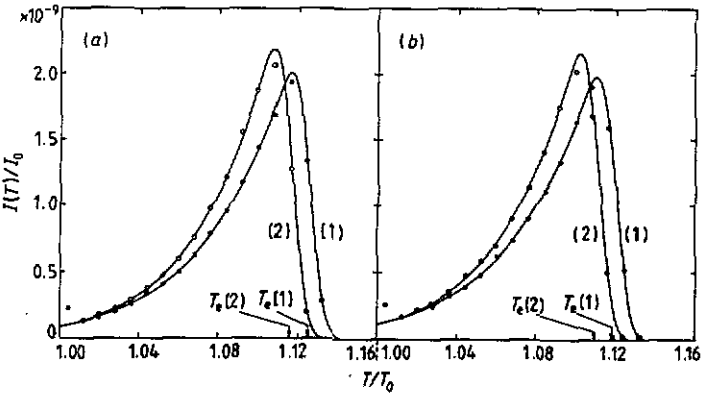

Figure 2. TSC peaks obtained for discrete trap level (a) and uniform distribution of traps (b): $\tau_0\beta/T_0 = 10^{-10}$; $\tau_{t0}\beta/T_0 = 10^{-12}$ (a), 5×10^{-13} (b); $\nu_0 T_0/\beta = 10^{15}$ (a), 5×10^{14} (b); $\varepsilon_t/kT_0 = 30$; $T_c/T_0 = 5$ (b); $a = -1.5$ (1), 1.5 (2); $b = 2$ (a), 0 (b); $N = 10^3$.

present case, the initial TSC rise is affected more strongly by the value of a than by the form of the trap distribution. The results given in figure 2(a) correspond to coulombic trapping centres, while the others correspond to neutral centres. The comparison of the curves denoted by (1) in figures 1(b) and 2(a) shows that the TSC course is almost independent of the kind of trapping centres (i.e. of the value of the parameter b). The most significant deviations between both curves occur near their maxima, and do not exceed 2%.

Figure 3 presents the time evolution of the total carrier density

$$n_{tot}(z, t) = n(z, t) + n_t(z, t)$$

in the sample for the uniform trap distribution. For the values of the parameters assumed here we have $\Theta(t) \simeq 10^{-10}$ to 10^{-8}, which implies that $n_{tot}(z, t) \simeq n_t(z, t)$. The free- and trapped-carrier densities cannot be calculated separately because of the small values of

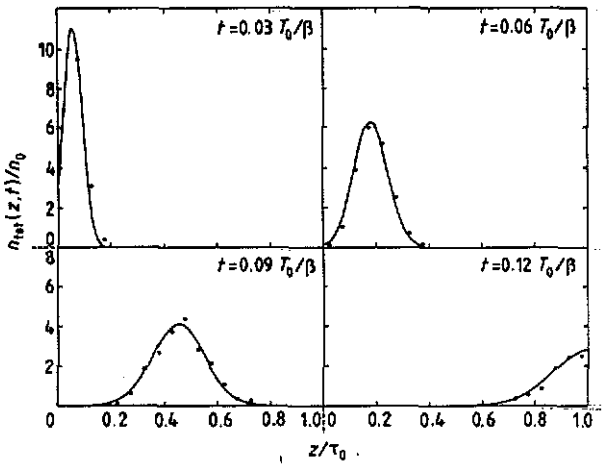

Figure 3. Spatial carrier distribution for several times obtained numerically (points) and calculated from equations (29) and (30) (full curves) for uniform trap distribution. The parameters are as in figure 2(*b*) (curve 1).

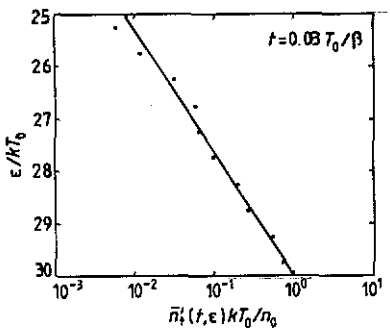

Figure 4. Energetic distribution of carriers obtained numerically (points) and calculated as described in the text (full line) for uniform distribution of traps. The parameters correspond to those from figure 2(*b*) (curve 1).

$n(z, t)$. Despite some fluctuations of the numerical results, it seems that the shape of the carrier packet is nearly Gaussian, except for slight deviations at its front and tail. The drift velocity of the carrier packet increases in time, which is a specific feature of non-isothermal transport.

Figure 4 shows the energetic distribution of the trapped carriers $n_t'(z, t, \varepsilon)$, averaged over the sample thickness, for the uniform distribution of traps. Assuming full thermal equilibrium between free and trapped carriers, one should expect that $\overline{n_t'}(t, \varepsilon) \propto \exp[\varepsilon/kT(t)]$ (cf. equations (2) and (4)). The proportionality constant in this relationship may be easily calculated, provided that carrier neutralization at the collecting electrode is negligible up to moment t. It is seen that the energetic distribution of the trapped carriers does not differ remarkably from the equilibrium distribution, through the dispersion of the numerical results is considerable for shallower traps.

5. Conclusions

In this paper, we have derived formulae describing the TSC for the case of multiple-trapping quasi-equilibrium carrier transport. We have also verified the analytical results by Monte Carlo calculations. The agreement is quite satisfactory, provided that carrier

thermalization is sufficiently quick. As far as possible applications of the theory are concerned, the following points should be re-emphasized:

(i) The shape and the position of the TSC peak are determined mainly by the maximum trap depth, as well as by the form of the trap distribution and the temperature dependence of the free-carrier mobility. In order to obtain any information about the trap distribution, the temperature dependence of the free-carrier mobility must be known *a priori*.

(ii) Both the initial TSC rise and the dependence of the TSC maximum on the $E/\beta d$ ratio enable us to calculate the same parameters, characterizing carrier trapping and transport.

(iii) In principle, the considered TSC technique and the TOF method are equivalent in the sense that they allow one to determine identical microscopic parameters.

Finally, it should be noted that similar TSC peaks can occur for hopping carrier transport with a single transition rate [20]. At present, the theoretical description of the TSC due to hopping transport is incomplete. This makes it difficult to discriminate between multiple-trapping and hopping transport modes and may introduce some ambiguity in the interpretation of experimental results.

Acknowledgments

The author wishes to thank Professor B Jachym for his kind interest in the work and Dr J Rybicki for critical reading and improving the manuscript.

Appendix 1. TSC for uniform initial distribution of carriers

We shall assume formally that the general solution of equation (26) is determined on the whole y axis. The solution can then be expressed by the Poisson integral (e.g. [26]):

$$n^*(y,\xi) = \frac{1}{2(\pi\xi)^{1/2}} \int_{-\infty}^{+\infty} n^*(y',0) \exp\left(-\frac{(y-y')^2}{4\xi}\right) dy'. \tag{A1.1}$$

For uniform carrier generation, the initial carrier distribution is given by $n(z,0) \simeq n_0\Theta(0)$ (cf. section 2.3), which implies that $n^*(y,0) \simeq n_0$ for $0 \leqslant y \leqslant \tau_0$. One can assume additionally that $n^*(y,0) = 0$ for $y < 0$ and $y > \tau_0$. Thus, making use of equation (A1.1) and returning to z and t variables, we obtain the expression for the free-carrier density:

$$n(z,t) = \frac{n_0\Theta(t)}{2}\left[\operatorname{erf}\left(\frac{z-\zeta(t)}{2\xi^{1/2}(t)}\right) + \operatorname{erf}\left(\frac{\tau_0 - z + \zeta(t)}{2\xi^{1/2}(t)}\right)\right]. \tag{A1.2}$$

The trapped-carrier density is determined by the formula $n_t(z,t) \simeq n(z,t)[1-\Theta(t)]/\Theta(t)$. The TSC can be calculated by inserting expression (A1.2) into equation (8). Assuming that $\xi^{1/2}(t)/\zeta(t) \ll 1$, after some transformations one gets

$$I(t) = \frac{I_0\Theta(t)u(t)}{2}\left\{\left(1-\frac{\zeta(t)}{\tau_0}\right)\left[1+\operatorname{erf}\left(\frac{\tau_0-\zeta(t)}{2\xi^{1/2}(t)}\right)\right] + \frac{2}{\tau_0}\left(\frac{\xi(t)}{\pi}\right)^{1/2} \times \exp\left(-\frac{[\tau_0-\zeta(t)]^2}{4\xi(t)}\right)\right\}. \tag{A1.3}$$

One can note that $I_{in}(t) = I_0\Theta(t)u(t)$, similarly as for surface carrier generation. At the time τ_e given by equation (33), TSC drops nearly to zero.

Appendix 2. The functions $\Theta(T)$, $\tau_s(T)$, $\zeta(T)$ and $\xi(T)$ for the model trap distributions

Let us consider first the case of a single trapping level (38). From equations (4), (14), (15), (36) and (37) we find immediately that

$$\Theta(T) \simeq \tau_{t0}\nu_0(T/T_0)^{3/2}\exp(-\varepsilon_t/kT) \qquad \Theta(T) \ll 1 \tag{A2.1}$$

$$\tau_s(T) = (1/\tau_{t0}\nu_0^2)(T/T_0)^{b-7/2}\exp(2\varepsilon_t/kT). \tag{A2.2}$$

Then, from equations (24), (34) and (35) we obtain

$$\zeta(T) = \frac{\tau_{t0}\nu_0}{\beta}\int_{T_0}^{T}\left(\frac{T'}{T_0}\right)^{a+3/2}\exp\left(-\frac{\varepsilon_t}{kT'}\right)dT' = \frac{\tau_{t0}\nu_0 T_0}{\beta}\left(\frac{\varepsilon_t}{kT_0}\right)^{a+5/2}$$

$$\times\int_{\varepsilon_t/kT}^{\varepsilon_t/kT_0}\frac{\exp(-s')}{(s')^{a+7/2}}ds' \tag{A2.3}$$

where the new variable $s' = \varepsilon_t/kT'$. Integrals of this form are frequently encountered in TSC theory and can be calculated approximately with the aid of the asymptotic expansion (e.g. [32])

$$\int_s^\infty\frac{\exp(-s')}{(s')^q}ds' \simeq \exp(-s)g(s) \qquad s \gg 1 \tag{A2.4}$$

where the function

$$g(s) = \sum_{m=0}^{n}\frac{(-1)^m\Gamma(q+m)}{\Gamma(q)s^{q+m}} \tag{A2.5}$$

with $\Gamma(\ldots)$ the Euler gamma function. This formula can be easily derived by successive integrations by parts. If $\varepsilon_t \gg kT$ and T is not too close to T_0, the upper limit in the last integral in (A2.3) can be replaced by infinity and only the first term of expansion (A2.5) can be taken. Thus, we get

$$\zeta(T) \simeq (\tau_{t0}\nu_0 kT_0^2/\varepsilon_t\beta)(T/T_0)^{a+7/2}\exp(-\varepsilon_t/kT). \tag{A2.6}$$

In an analogous way, we find from equations (25), (34) and (35) that

$$\xi(T) \simeq (\tau_{t0}^2\nu_0 kT_0^2/\varepsilon_t\beta)(T/T_0)^{2a+b+3}\exp(-\varepsilon_t/kT). \tag{A2.7}$$

Let us consider now the case of the power trap distribution (39). Then, equations (4), (14), (36) and (37) give

$$\Theta^{-1}(T) \simeq \frac{(c+1)}{\tau_{t0}\nu_0(kT_c)^{c+1}}\left(\frac{T}{T_0}\right)^{-3/2}\int_{\varepsilon_t^0}^{\varepsilon_t}(\varepsilon_t-\varepsilon)^c\exp\left(\frac{\varepsilon}{kT}\right)d\varepsilon$$

$$= \frac{(c+1)}{\tau_{t0}\nu_0}\left(\frac{T_0}{T_c}\right)^{c+1}\left(\frac{T}{T_0}\right)^{c-1/2}\exp\left(\frac{\varepsilon_t}{kT}\right)\int_0^{T_c/T}r^c\exp(-r)\,dr \tag{A2.8}$$

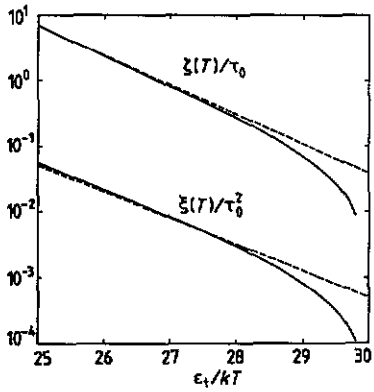

Figure A.1. Functions $\zeta(T)$ and $\xi(T)$ for uniform distribution of traps calculated from exact (full curves) and approximate (broken curves) formulae: $\tau_0\beta/T_0 = 10^{-10}$, $\tau_{t0}\beta/T_0 = 5 \times 10^{-13}$, $\nu_0 T_0/\beta = 5 \times 10^{14}$, $\varepsilon_t/kT_0 = 30$, $T_c/T_0 = 5$, $a = -1.5$, $b = 0$.

for $\Theta(T) \ll 1$ where $kT_c = \varepsilon_t - \varepsilon_t^0$ and $r = (\varepsilon_t - \varepsilon)/kT$. Assuming that $T_c \gg T$ and making use of the formula

$$\int_0^\infty r^c \exp(-r)\,dr = \Gamma(c+1) \tag{A2.9}$$

we find

$$\Theta(T) \simeq \frac{\tau_{t0}\nu_0}{\Gamma(c+2)}\left(\frac{T_c}{T_0}\right)^{c+1}\left(\frac{T}{T_0}\right)^{-c+1/2}\exp\left(-\frac{\varepsilon_t}{kT}\right). \tag{A2.10}$$

In similar manner, from equations (4), (15), (36) and (37) we obtain

$$\tau_s(T) \simeq \frac{\Gamma(c+2)}{\tau_{t0}\nu_0^2}\left(\frac{T_0}{2T_c}\right)^{c+1}\left(\frac{T}{T_0}\right)^{b+c-5/2}\exp\left(\frac{2\varepsilon_t}{kT}\right). \tag{A2.11}$$

The calculation of the functions $\zeta(T)$ and $\xi(T)$ proceeds in identical way as for a monoenergetic trapping level. The final formulae are

$$\zeta(T) \simeq \frac{\tau_{t0}\nu_0 kT_0^2}{\Gamma(c+2)\varepsilon_t\beta}\left(\frac{T_c}{T_0}\right)^{c+1}\left(\frac{T}{T_0}\right)^{a-c+5/2}\exp\left(-\frac{\varepsilon_t}{kT}\right) \tag{A2.12}$$

$$\xi(T) \simeq \frac{\tau_{t0}^2\nu_0 kT_0^2}{\Gamma^2(c+2)2^{c+1}\varepsilon_t\beta}\left(\frac{T_c}{T_0}\right)^{2c+2}\left(\frac{T}{T_0}\right)^{2a+b-2c+1}\exp\left(-\frac{\varepsilon_t}{kT}\right). \tag{A2.13}$$

The accuracy of formulae (A2.12) and (A2.13) is illustrated by figure A.1. The corresponding plots for a discrete trap level are very similar and are not presented here. Also, the plots of the functions $\Theta(T)$ and $\tau_s(T)$ are not shown since their values calculated from the approximate and exact formulae are almost the same.

Appendix 3. The algorithm for calculating Δt_r from equation (51)

Making use of equations (4), (34) and (37), we rewrite equation (51) in the form

$$\int_s^{s_0} \frac{\exp(-s')}{(s')^{4-b}}\,\mathrm{d}s' = P \tag{A3.1}$$

where

$$s_0 = \varepsilon/k(T_0 + \beta t_r) \tag{A3.2}$$

$$s = \varepsilon/k[T_0 + \beta(t_r + \Delta t_r)] \tag{A3.3}$$

$$P = -(\beta/\nu_0 T_0)(kT_0/\varepsilon)^{3-b} \ln(X'''). \tag{A3.4}$$

Thus, the problem consists of calculating the s value, determined by equation (A3.1). The time Δt_r is obtained next from the formula

$$\Delta t_r = (\varepsilon/\beta k)(1/s - 1/s_0) \tag{A3.5}$$

which results from equations (A3.2) and (A3.3).

To calculate the integral (A3.1), we utilize the asymptotic expansion (A2.4) with (A2.5). In the present calculations, the minimum value of s exceeded 20. Therefore, a relatively small number of terms in expansion (A2.5) was needed to ensure good accuracy ($n = 8$ and 10 for $b = 0$ and 2, respectively). After simple transformations, from equation (A3.1) one obtains

$$s \simeq \ln[g(s)/Q] \tag{A3.6}$$

where

$$Q = P + \exp(-s_0)g(s_0). \tag{A3.7}$$

Equation (A3.6) is easy to solve by the iteration method (e.g. [33]). Since the absolute value of the derivative

$$\mathrm{d}\ln[g(s)/Q]/\mathrm{d}s \simeq -(4-b)/s \qquad s \gg 1 \tag{A3.8}$$

is much less than unity, the convergence is very fast. To obtain the formula, determining the initial value s^* for the iteration procedure, one can note that the root of equation (A3.6) is an almost linear function of $\ln(Q)$. Solving this equation for some range of the parameter Q and using the least-squares method, we get

$$s^* = -9.21 - 0.902\ln(Q) \tag{A3.9}$$

and

$$s^* = -4.85 - 0.949\ln(Q) \tag{A3.10}$$

for $b = 0$ and $b = 2$, respectively. These formulae represent the best fit in the range $15 \leqslant s^* \leqslant 65$ and their accuracy is better than 5%. In some calculations, more exact formulae for s^*, involving also higher powers of $\ln(Q)$, were used.

The above procedure is not optimal when $s_0 - s \ll 1$. In such a case, because of a partial cancellation of the terms in equation (A3.5), equation (A3.6) must be solved with very high accuracy. A more convenient procedure is then as follows. Introducing

the notation $\Delta s = s_0 - s$ and expanding the expression on the LHS of equation (A3.1) in a Taylor series, one obtains

$$\Delta s + [1 + (4-b)/s_0]\,\Delta s^2/2 + [1 + 2(4-b)/s_0 + (4-b)(5-b)/s_0^2]\,\Delta s^3/6 \simeq R \qquad \Delta s \ll 1 \tag{A3.11}$$

where

$$R = P s_0^{4-b} \exp(s_0). \tag{A3.12}$$

Inverting the power series (see e.g. [34]) we get the formula

$$s \simeq s_0 - R + [1 + (4-b)/s_0]\,R^2/2 - [1 + 2(4-b)/s_0 + (4-b)(7-2b)/2s_0^2]\,R^3/3 \qquad R \ll 1 \tag{A3.13}$$

which represents the approximate solution of equation (A3.1). In the program, in order to select between both methods, parameter R given by equation (A3.12) is first calculated. If $R < 0.01$, which implies that $\Delta s \ll 0.01$, the formula (A3.13) is used; otherwise equation (A3.6) is solved.

References

[1] Hearing R R and Adams E N 1960 *Phys. Rev.* **117** 451
[2] Cowell T A T and Woods J 1967 *Br. J. Appl. Phys.* **18** 1045
[3] Simmons J G and Taylor G W 1972 *Phys. Rev.* B **5** 1619
[4] Simmons J G, Taylor G W and Tam M C 1973 *Phys. Rev.* B **7** 3714
[5] Scher H and Montroll E W 1975 *Phys. Rev.* B **12** 2455
[6] Noolandi J 1977 *Phys. Rev.* B **16** 4466
[7] Noolandi J 1977 *Phys. Rev.* B **16** 4474
[8] Schmidlin F W 1977 *Phys. Rev.* B **16** 2362
[9] Rudenko A I and Arkhipov V I 1982 *Phil. Mag.* B **45** 177
[10] Rudenko A I and Arkhipov V I 1982 *Phil. Mag.* B **45** 209
[11] Arkhipov V I and Rudenko A I 1982 *Phil. Mag.* B **45** 189
[12] Samoć M and Samoć A 1980 *Phys. Status Solidi* a **57** 667
[13] Plans J, Zieliński M and Kryszewski M 1981 *Phys. Rev.* B **23** 6557
[14] Tomaszewicz W and Jachym B 1984 *J. Non-Cryst. Solids* **65** 193
[15] Schrader S and Kryszewski M 1985 *Phys. Status Solidi* a **91** 243
[16] Tomaszewicz W 1985 *Phil. Mag.* B **52** 881
[17] Tomaszewicz W, Rybicki J, Jachym B, Chybicki M and Feliziani S 1990 *J. Phys.: Condens. Matter* **2** 3311
[18] Rybicki J, Feliziani S, Tomaszewicz W, Jachym B and Chybicki M 1991 *J. Phys.: Condens. Matter* **3** 4229
[19] Chen I 1976 *J. Appl. Phys.* **47** 2988
[20] Plans J, Baltá Calleja F J, Zieliński M and Kryszewski M 1983 *Phil. Mag.* B **48** 289
[21] Stasiak M, Jeszka J K, Zieliński M, Plans J and Kryszewski M 1980 *J. Phys. D: Appl. Phys.* **13** L221
[22] Schrader S 1983 *PhD Thesis* Akademie der Wissenschaften der DDR Berlin
[23] Samoć M, Samoć A, Sworakowski J and Karl N 1983 *J. Phys. C: Solid State Phys.* **16** 171
[24] Samuel L M, Sanda P N and Miller R D 1989 *Chem. Phys. Lett.* **159** 227
[25] Samuel L M, Sanda P N, Miller R D and Thompson D 1990 *Mol. Cryst. Liq. Cryst.* **183** 211
[26] Band W 1959 *Introduction to Mathematical Physics* (Princeton, NJ: Van Nostrand) p 112
[27] Bube R H 1974 *Electronic Properties of Crystalline Solids* (New York: Academic) ch 8
[28] Kivits P and Hagebeuk H J L 1977 *J. Luminesc.* **15** 1
[29] Marshall J M 1977 *Phil. Mag.* **36** 959
[30] Silver M and Cohen L 1977 *Phys. Rev.* B **15** 3276
[31] Dwass M 1970 *Probability and Statistics. An Undergraduate Course* (New York: Benjamin) p 274

[32] Chen R and Kirsh Y 1981 *Analysis of Thermally Activated Processes* (Oxford: Pergamon) p 322
[33] Scarborough J B 1962 *Numerical Mathematical Analysis* 5th edn (Baltimore: Johns Hopkins Press) p 206
[34] Dwight H B 1957 *Tables of Integrals and Other Mathematical Data* 3rd edn (New York: Macmillan) p 11